CONF-900216--3

NUCLEAR WEAPON RADIATION EFFECTS ON A SPACE BASED INTERCEPTOR WEAPON PLATFORM *

J. O. Johnson, M. S. Smith, and R. T. Santoro

Engineering Physics and Mathematics Division
Post Office Box 2008
Oak Ridge National Laboratory†
Oak Ridge, Tennessee 37831-6363

CONF-900216--3
DE89 016258

* This work was sponsored by the Air Force Weapons Laboratory.

† Operated by Martin Marietta Energy Systems, Inc., under contract DE-AC05-84OR21400, U.S. Department of Energy

---

NUCLEAR WEAPON RADIATION EFFECTS ON A SPACE BASED INTERCEPTOR WEAPON PLATFORM

J. O. Johnson, M. S. Smith, and R. T. Santoro

Engineering Physics and Mathematics Division
Oak Ridge National Laboratory
Oak Ridge, Tennessee 37831

Electronic equipment, especially modern integrated circuits, will undergo an alteration of the electrical properties of the active components when exposed to various radiation environments. The changes in the electrical properties can result in degradation of circuit performance or temporary/permanent circuit failure. Studies of the nuclear environment and its effects on space based systems and shielding are required so that the benefits of added shielding can be determined and application methods, materials, and shield designs can be identified which optimize the shields survivability and nuclear mitigation capability.

The purpose of this study[1-3] was to determine the dose to the various electronic components and sensitive areas (fuel tanks) of a representative Space Based Interceptor (SBI) weapon platform due to an exo-atmospheric nuclear weapon detonation. In particular, the damage resulting from incident neutrons, gamma-rays, and X-rays generated by the weapon detonation was assessed for the critical electronic components and for materials whose chemical/physical properties might degrade. To perform this analysis, a three dimensional ORNL computer model of a SBI weapon platform (Figure 1) was devised to estimate the effects of natural and nuclear weapon radiation on the external surfaces and materials and on the internal components. It should be noted that the SBI weapon platform used in this study represents the author's concept of such a system.

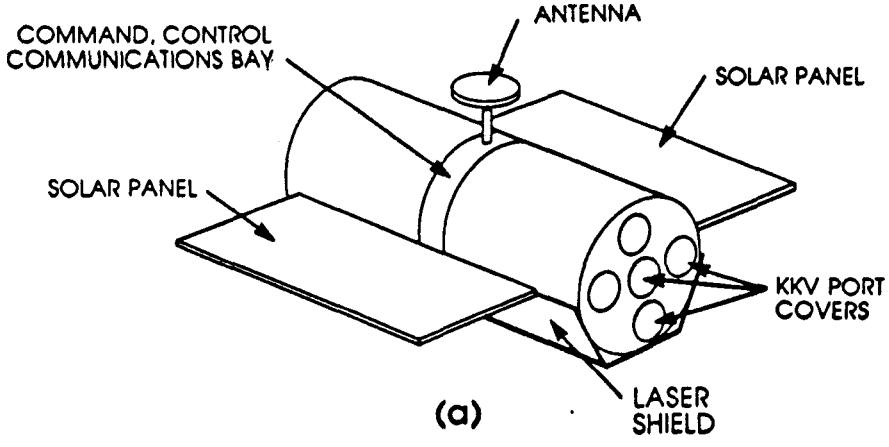

Figure 1. Calculational Model of the
Space Based Interceptor Weapon Platform

The ORNL model of a SBI weapon platform is a cylindrical shell comprised of two Kinetic Kill Vehicle (KKV)–fuel tank modules connected by a Command, Control, and Communications (C^3) bay. Each module contains five KKV–launch tube assemblies and four fuel tanks. Power is supplied to the platform by solar panels shown in the deployed position in Figure 1. A single antenna is shown, but it is recognized that other antennae and sensors may also exist on an actual platform design. A laser weapon shield covers the earth–exposed surfaces for protection against illumination by ground based laser weapons. A KEW shield was not included as part of the platform due to uncertainty in the positioning of these shields, i.e., directional or full coverage, and also to obtain data on the radiation response of components and surface materials and hardening requirements for the platform itself. The electronic circuits are housed in two concentric ring assemblies in the C^3 bay. At the center of the module is a "critical components" box. The cylindrical ring assemblies and the box are thin walled hollow assemblies that can be filled with detailed models of electronic circuitry, homogenized materials representative of those comprising the electronic packages, and also additional local shielding should it be necessary to further minimize the effects of radiation. Ten identical KKVs are modeled in their appropriate locations inside the platform. The principal components of each kill vehicle include the warhead, sensors, computers, fuel tank, and rocket motor.

The neutron and gamma–ray source spectra employed in this study include a deuterium–tritium fusion reaction spectrum, a pure ^{235}U fission spectrum and a prompt fission gamma–ray spectrum. An actual weapon spectrum may be a combination of fusion and fission components, which can be modeled using the spectra in this study. The gamma–ray contribution from the coupled sources may vary between approximately 33% (pure fusion) and approximately 95% (pure fission). To examine the nuclear weapon X–ray radiation effects, calculations of blackbody X–rays at a variety of temperatures were considered. As the temperature of the blackbody radiator increases, the emission spectrum hardens. The blackbody X–ray calculations were performed so that the effects of an arbitrary weapon X–ray spectrum can be created. To allow construction of a blackbody radiation spectrum representative of a nuclear weapon detonation, temperatures (kT) of 2, 5, 10, and 20 keV were used. Surface loadings in the range of 1–10 cal/cm^2 were considered.

To accommodate the directional source spectra incident on the SBI platform from a nuclear detonation, three scenarios were considered in the analysis. The first scenario modeled the nuclear detonation directly above the SBI platform, the second scenario modeled the nuclear detonation directly in front of the SBI platform, and the third scenario modeled the nuclear detonation incident on the top and front face of the platform at a 45 degree angle. The nuclear weapon detonation was modeled such that the incident radiation spectra could be assumed monodirectional.

Analysis routines were written to calculate the dose to those areas of the platform which contain electronic components or materials which may be sensitive to radiation damage. To accommodate directional source spectra, 68 different detector regions were identified. The term detector in this context is used to identify a region in the radiation transport geometry model for which a response is desired. In particular, the C^3 Bay contains 15 detector regions. These include the critical electronic component box in the center of the C^3 Bay, six angular segments for the inner electronic bay ring, and eight angular segments for the outer electronic bay ring. The computer region, sensor region, and fuel tank were modeled for all ten KKVs onboard the platform. The solar panels have been modeled as two separate detector regions, with each panel subdivided into five additional detector regions

to calculate dose profiles and identify potential surface phenomenology, i.e. blow off, melting, etc. The antenna has been modeled as a separate detector region and it also has been subdivided into five additional detector regions to calculate dose profiles and identify potential surface phenomenology. Finally, the eight SBI platform fuel tanks have been modeled as separate detector regions. The Hydrazine fuel was considered because of possible radiation–induced chemical degradation.

The MORSE code was used to perform all neutron and gamma–ray calculations. MORSE is a multipurpose Monte Carlo transport code whose features include the transport of either neutrons or gamma–rays, the incorporation of multigroup cross sections, and a three dimensional combinatorial geometry package. The EGS4 code was used to perform all X–ray calculations. EGS4 is a three-dimensional multimedia Monte Carlo transport code which takes into account all important physical processes for the transport of electrons, positrons, or gamma–rays, and also can operate with the combinatorial geometry package.

The MORSE code results were obtained from 500,000 particle histories (100 batches of 5000 particles each) yielding excellent fractional standard deviations (fsd) in the regions of interest. To reduce computational effort and improve the accuracy of the results, the EGS4 calculations were divided into source spectra incident on the platform body and source spectra incident on the solar panels. For the platform body, the EGS4 calculations analyzed 30 batches of 10,000 particles and for the solar panels, the calculations analyzed 10 or 20 batches of 2,000 particles depending on the temperature of the incident X–ray spectrum. With both MORSE and EGS4, only the weapon detonation directly above the platform was analyzed for the solar panels. The principal reason for this was because the surface area irradiated by the detonation at a 45 degree angle was similar to that for the detonation directly above the platform, and the surface area irradiated by the detonation directly in front of the platform was insignificant.

The neutron and gamma-ray results shown in Tables 1 and 2 have been normalized to a one kiloton output of neutrons and gamma–rays, assuming 100% yield efficiency. This assumption results in 1.88×10^{23} prompt fission neutrons and 1.06×10^{24} prompt fission gamma–rays, or 1.49×10^{24} fusion neutrons, per kiloton of yield. The tabulated data are in units of rads(material)$\cdot m^2$/kTon. The dose received by a particular component can be quickly assessed by multiplying by the device yield and dividing by the square of the separation distance. Note that the factor of 4π has already been included in the tabulated data. The total dose level in a component is a summation of the contributions from the primary and secondary particles. For example, a 100 kTon fission device detonated at 1 kilometer above the SBI platform generates a total dose in the central instrument box of 26.5 krad(Si) from primary neutrons, primary gamma rays (prompt gamma rays), and secondary gamma rays.

The results in Tables 1 and 2 can also be normalized to X–ray surface loadings. If it is assumed that 75% of the energy from a detonation is in the form of X–rays, then device yields may be converted to surface loadings (using 10^{12} cal/kT). For example, the 1962 Starfish event had a yield of 1.4 MT, of which 1 MT was fission yield. At a distance of 91.4 km from the device, the X–ray surface loading is 1 cal/cm^2. Using this distance and yield, coupled with the source spectra given in these tables, total dose and dose rate can be calculated for the SBI model. The total dose in the C^3 bay critical box is 136 rads(Si). The dose rate for a 40 nanosecond pulse width, $\dot{\gamma}$, is 1.7×10^9 rads(Si)/sec. Consequently, the limiting factor with respect to damage is the dose rate.

Electronic devices can be hardened to withstand high levels of neutron fluence and dose. Therefore, the gamma dose level and dose rate predominates in terms of electronic component shielding. An actual weapon spectrum may be a combination of fusion and fission components, which can be modeled using the spectra in Reference 3. By adding some high–Z material around the central instrument bay, significant reductions in gamma dose may be obtained.

The X–ray results presented in Table 3 have been normalized to one X–ray/cm^2 assuming 100% yield efficiency. To obtain total dose (in rads) for a 1 cal/cm^2 exterior wall loading, the results in Table 3 must be multiplied by 4.86×10^{15} X–rays/cm^2 for a 2 keV blackbody source, 1.94×10^{15} X–rays/cm^2 for a 5 keV blackbody source, 9.67×10^{14} X–rays/cm^2 for a 10 keV blackbody source, and 4.82×10^{14} X–rays/cm^2 for a 20 keV blackbody source. The dose to the sensitive components within the exterior hull of the platform was not sufficient to cause any damage at a 1 cal/cm^2 exterior wall loading of X–rays. At higher wall loadings, some of the KKV computers and sensors begin to receive doses large enough to cause damage. Furthermore, the majority of the dose to the internal components of the SBI platform came from blackbody devices with temperatures greater than 10 keV. The low temperature devices will yield a higher flux of X–rays, but the incident energy will be insufficient to cause permanent damage to the internal electronic components.

The analysis presented in this work focused on the total dose (in units of rads or rads · cm^2/X-ray) received by the various components on board the SBI weapon platform without regard to the rate at which the dose was received. As stated above, generally the total dose to the sensitive components within the exterior hull of the platform was not sufficient enough to cause any damage at a 1 cal/cm^2 exterior wall loading. However, a typical weapon detonation releases the X–ray radiation in a pulse. Therefore, if a 40 nanosecond pulse width is assumed, all of the total dose results would have to be multiplied by 2.5×10^7 sec^{-1} to obtain the dose rate ($\dot{\gamma}$) results. This would yield dose rates to the sensitive components in the range of 10^8–10^{12} rads/sec which could be large enough to cause damage. Consequently, the dose rate becomes the primary mode of failure even though the total dose is not large enough to cause any damage to the sensitive components. In this case, additional shielding around the sensitive components would be required.

REFERENCES

J. M. Barnes, R. T. Santoro, J. O. Johnson, J. D. Drischler, T. A. Gabriel, and M. S. Smith, "Shield Optimization Program, Part II: Effects of Van Allen Belt Radiation on SDI Weapon Platforms," ORNL/TM-10957, Oak Ridge National Laboratory, Oak Ridge, Tennessee.

J. O. Johnson, T. A. Gabriel, J. M. Barnes, J. D. Drischler, M. S. Smith, and R. T. Santoro, "Shield Optimization Program, Part III: Effects of X-Ray Radiation From Nuclear Weapons on SDI Weapon Platforms," ORNL/TM-10985, Oak Ridge National Laboratory, Oak Ridge, Tennessee.

M. S. Smith, J. O. Johnson, T. A. Gabriel, J. M. Barnes, J. D. Drischler, and R. T. Santoro, "Shield Optimization Program, Part IV: Effects of Neutron and Gamma–Ray Radiation From Nuclear Weapons on SDI Weapon Platforms," ORNL/TM-10975, Oak Ridge National Laboratory, Oak Ridge, Tennessee.

Table 1. Neutron and Gamma Dose Levels in the SBI Weapon Platform from the Deuterium–Tritium Fusion Source Located Directly Above the SBI Platform (rads·m²/kTon)

Detector Region	Neutron	Secondary Gamma
C^3 Critical Box	1.406+09[a] ± 3.7[b]	7.588+08 ± 7.4
C^3 Inner Ring	1.927+09 ± 2.3	1.055+09 ± 6.4
C^3 Outer Ring	2.144+09 ± 2.7	9.843+08 ± 5.8
KKV Computer	2.701+09 ± 2.2	9.309+08 ± 6.3
KKV Sensor	2.531+09 ± 2.0	9.496+08 ± 6.2
Solar Panel Surface	2.057+08 ± 1.3	2.322+07 ± 5.6
Antenna Surface	7.113+08 ± 3.4	2.038+08 ± 13.4
KKV Fuel Tank	9.332+10 ± 1.4	1.512+09 ± 3.2
SBI Fuel Tank	3.277+11 ± 0.8	6.344+09 ± 1.8

[a]Read as 1.406×10^9.
[b]Percent Fractional Standard Deviation.

Table 2. Neutron and Gamma Dose Levels in the SBI Weapon Platform from the Fission Sources Located Directly Above the SBI Platform (rads·m²/kTon)

Detector Region	Neutron	Secondary Gamma	Prompt Gamma
C^3 Critical Box	1.659+07[a] ± 3.8[b]	1.738+07 ± 8.6	2.332+08 ± 3.4
C^3 Inner Ring	2.076+07 ± 2.4	2.240+07 ± 6.8	3.596+08 ± 2.5
C^3 Outer Ring	2.631+07 ± 2.6	2.192+07 ± 5.5	4.792+08 ± 3.0
KKV Computer	3.006+07 ± 2.2	2.426+07 ± 5.2	5.794+08 ± 2.7
KKV Sensor	2.801+07 ± 1.9	2.476+07 ± 5.7	5.458+08 ± 2.4
Solar Panel Surface	3.621+06 ± 1.0	4.799+05 ± 9.5	4.774+07 ± 2.1
Antenna Surface	7.738+06 ± 3.6	3.044+06 ± 10.2	1.894+08 ± 3.8
KKV Fuel Tank	4.786+09 ± 1.5	7.502+07 ± 3.5	1.084+09 ± 1.6
SBI Fuel Tank	1.295+10 ± 1.0	3.613+08 ± 1.9	4.050+09 ± 1.1

[a]Read as 1.659×10^7.
[b]Percent Fractional Standard Deviation.

Table 3. X-Ray Dose Levels in the SBI Weapon Platform from the Various Temperature Blackbody X-Ray Sources Located Directly Above the SBI Platform (rads-cm²/X-Ray)

Detector Region	Temperature of Blackbody Source 2 keV	5 keV	10 keV	20 keV
C^3 Critical Box	0.000+00 ± 0.0	2.748−17[a] ± 45.2[b]	7.931−15 ± 26.5	6.278−14 ± 9.7
C^3 Inner Ring	0.000+00 ± 0.0	9.171−17 ± 42.0	7.952−15 ± 13.8	7.949−14 ± 9.1
C^3 Outer Ring	4.423−18 ± 16.5	4.811−15 ± 6.6	6.820−14 ± 4.0	2.639−13 ± 3.2
KKV Computer	9.332−18 ± 13.7	1.010−14 ± 5.6	1.221−13 ± 3.9	4.131−13 ± 4.4
KKV Sensor	4.645−18 ± 12.1	7.879−15 ± 5.9	1.012−13 ± 3.6	3.553−13 ± 3.1
Solar Panel Surface	7.427−13 ± 0.5	9.185−13 ± 1.0	5.885−13 ± 2.9	5.081−13 ± 3.9
Antenna Surface	7.460−13 ± 1.6	1.554−12 ± 1.2	1.533−12 ± 1.9	1.331−12 ± 2.5
KKV Fuel Tank	3.576−18 ± 13.1	3.260−15 ± 6.6	3.471−14 ± 3.4	1.443−13 ± 3.0
SBI Fuel Tank	7.781−18 ± 5.2	4.989−15 ± 1.6	4.490−14 ± 1.3	1.608−13 ± 0.8

[a]Read as 2.748×10^{-17}.
[b]Percent Fractional Standard Deviation.